A METHOD TO REFINE MAIN FIELD MODELING

I. Wardinski[1] **and R. Holme**[2]

[1]GeoForschungsZentrum Potsdam Sec. 2.3 *Earth's Magnetic Field*, Potsdam, Germany
[2]Dep. of Earth's and Ocean Sciences, University of Liverpool, UK

ABSTRACT

So far, time dependent main field models do not consider external field variation in terms of spherical harmonics. In the CM4 [1] external field variations are modelled as functions of geomagnetic activity indices like the DST index. Such parameterisation boosts the model complexity, but disregarding external field variation bears the risk that such variation is interpreted as secular variation. Here we present a simple method to avoid this fault behaviour.

In order to estimate the Gauss coefficients from geomagnetic observations a least-squares scheme is applied. Here, a crucial point is the set up of the error covariance matrix. Up to now the error has been treated as isotropic. In this study we apply a method developed by [2; 3], which allow for error covariances to regard external field variation. In principal, such a more sophisticated modelling of the error correlations produce an improved model. A comparison between these methods are given and results discussed.

Key words: Main field modelling, time–dependent.

1. INTRODUCTION

The PUFM [4] is a continuous model of the geomagnetic field and its secular variation for the period 1980 to 2000. In this approach the magnetic potential V is decomposed into spherical harmonics up to degree and order 15.

$$V = a \sum_{l,m} \left(\frac{a}{r}\right)^{l+1} (g_l^m \cos m\phi + h_l^m \sin m\phi) \times \mathrm{P}_l^m(\cos\theta) \quad (1)$$

and expand each harmonic coefficient g_l^m on a basis of cubic B–Splines $M_n(t)$ in time [5]

$$g_l^m(t) = \sum_{n=1}^{N} g_l^{mn}\, M_n(t)\,. \quad (2)$$

Further, our model is constrained to fit satellite field models in the end points **MAGSAT and ØRSTED** for 1980.0 and 2000.0. The solution $\mathsf{m} = \{g_1^{00}, g_1^{10}, h_1^{10}, \ldots\}$ of this least square problem is given by

$$\mathsf{m} = (\mathbf{A}^\mathsf{T} {\mathbf{C_e}}^{-1} \mathbf{A} + {\mathbf{C_m}}^{-1} + \Gamma^{-1})^{-1} \mathbf{A}^\mathsf{T} {\mathbf{C_e}}^{-1} \gamma\,, \quad (3)$$

where $\mathbf{C_m}$ is the a priori model covariance matrix (spatial and temporal smoothness of the model), Γ controls the departure of the model from the satellite field model and γ the data vector. The data are annual differences of observatory annual or monthly means (secular variation estimates)

The solution is sought in an iterative re-weighting scheme comprising eight steps:

1. A initial model is computed weighting all data with the same uncertainty (5 nT/yr).
2. The deviations of the data from the initial model are calculated, and adopted as new weights for the data. Data with large scatter from the model are therefore down-weighted.
3. A model is derived from the newly (re-) weighted data set.
4. Data are discarded which deviate by more then 2 σ from the second model.
5. A interim model is derived from this reduced data set.

In steps 6 to 8 we generalized step 2 (the estimation of the data weighting) by further considering the covariance between the different field components (X,Y,Z) at each location, in order to allow for possible correlated errors. For example, in mid-latitudes, we might expect that the error would be dominated by the unmodelled signal from external field variations, in particular the ring current, leading to a particularly strong error correlation between the X and Z components.

In this study we discuss the different results of the model with no error correlation (the interim model) and the model, where we consider error correlation (the final model).

2. RESIDUALS ANALYSIS

The residuals between the interim model and the measurements in Niemegk (Fig.1a) are analysed by means of autocorrelation and cross correlation functions.

The autocorrelation function is defined by

$$A(\tau) = c \sum_{t=1}^{N-\tau} (x_t - \langle x_t \rangle)\,(x_{t+\tau} - \langle x_{t+\tau} \rangle)/(x_t - \langle x_t \rangle)^2\,, \tag{4}$$

where x_t is time series of the residuals, τ is the shift and $c = 1/(N-\tau)$. Variations with periods multiple of τ will have a local maximum in $A(\tau)$.

Apparently the dip at $\tau = 12$ in all curves of Fig.1b is due to the processing of the data, to derive the secular variation estimates. There are no further obvious peaks in. The cross correlation function is defined as

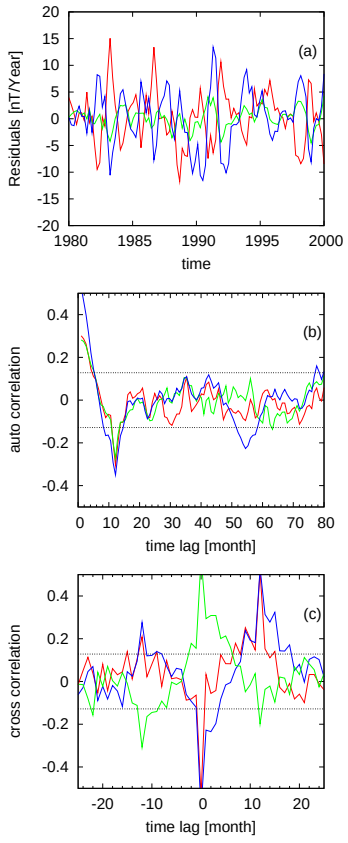

Figure 1: (a) Residuals between model and the secular variation estimates for Niemegk. Residuals for X (red), Y (green) and Z (blue) (**b**) Autocorrelation function of the residuals using the same line styles as for the residuals. (**c**) Cross-correlation functions of the residuals between $\dot{\mathrm{X}}$ and $\dot{\mathrm{Y}}$ (red), between $\dot{\mathrm{X}}$ and $\dot{\mathrm{Z}}$ (blue) and between $\dot{\mathrm{Y}}$ and $\dot{\mathrm{Z}}$(green). The horizontal black lines represent the 95 % significance level for not being white noise.

$$C(\tau) = c\,\frac{\sum_{t=1}^{N-\tau}(x_t - \langle x_t \rangle)(y_{t+\tau} - \langle y_{t+\tau} \rangle)}{\sqrt{(\sum_t (x_t - \langle x_t \rangle)^2)}\sqrt{(\sum_t (y_{t+\tau} - \langle y_t \rangle)^2)}}\,. \tag{5}$$

It shows the common correlations of two independent time series x_t and y_t.

The cross correlation function of the residuals against each other for Niemegk are shown in Fig.1c. The maxima at a lag of zero, which are evident in all graphs, indicate that the variation of the residual components are correlated or anti–correlated, respectively. This could mean that the effect of variations, i.e. the semi–annual variation, causes a increase of the residuals lets say in X and Y, what gives a correlation, an increase in the residuals of X and a decrease of the residuals of Y signify an anti–correlation. In detail; the residuals of $\dot{\mathrm{Y}}$ and $\dot{\mathrm{Z}}$ are correlated, $\dot{\mathrm{X}}$ and $\dot{\mathrm{Y}}$ are anti–correlated and $\dot{\mathrm{X}}$ and $\dot{\mathrm{Z}}$ are anti–correlated. The situation changes form observatory to observatory. This behaviour is mainly due to the different geometries of the ring current at different location and due to different interaction with the distinct magnetisation of the crust at each observatory site.

3. METHOD

In order to determine the Gauss coefficients we have to minimise the misfit

$$\mathsf{e}^{\mathsf{T}}\,{\mathbf{C_e}}^{-1}\mathsf{e}\,, \tag{6}$$

where C_e is the data error covariance matrix

$$(\mathbf{C_e})_{ij} = cov(\mathsf{e}_i, \mathsf{e}_j)\,, \tag{7}$$

and $\mathsf{e} = \gamma - \mathbf{A}\mathsf{m}$ the error vector. If the data error are uncorrelated, then the covariance matrix is diagonal, if not the inversion requires a factorisation of a sparse matrix whose dimension is the number of data. For simplicity, we consider the data errors to be correlated at the same site only, then the covariance matrix is a 3×3 matrix and can easily be inverted [2].

Linear algebra provides: the eigenvalue of a real symmetric matrix are real and orthogonal and if the eigenvectors ν and the eigenvalues λ are known, then the normal equations matrix can be derived as

$$\mathbf{A}^{\mathsf{T}}{\mathbf{C_e}}^{-1}\mathbf{A} = \mathbf{A}^{\mathsf{T}} \sum_i \lambda_i \nu_i \nu_i^{\mathsf{T}} \mathbf{A} \tag{8}$$

The eigenvectors and eigenvalues are computed from the covariance matrix of the residuals of each observatory site.

4. RESULTS

Figure 2 (a-c) show a comparison between the data and two models, one derived with the covariance matrix of uncorrelated data errors, and the other with the covariance matrix of correlated data errors for Niemegk observatory. Figure 2 (d-f) show the same comparison, but now in the three individual covariance directions. The same comparison as above for Gnangara observatory. The differences between both methods is particularly clear in $\dot{Y}$

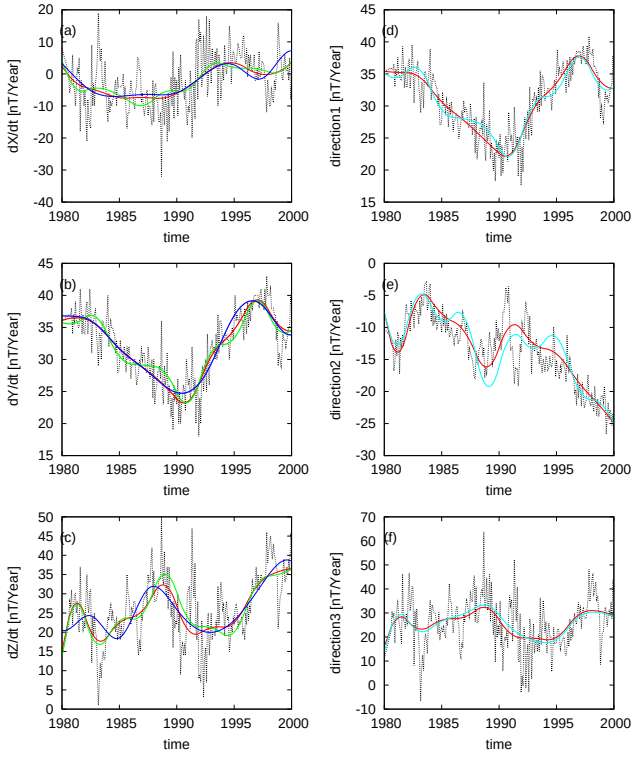

Figure 2: Sub-figures (a) – (c) show a comparison between data (black dashed line), the model with no error correlation (green), the model with error correlation (red) and the prediction of CM4 (blue) for Niemegk, the figures (d) – (f) on the right side show this comparison for the three individual covariance directions using the same line style.

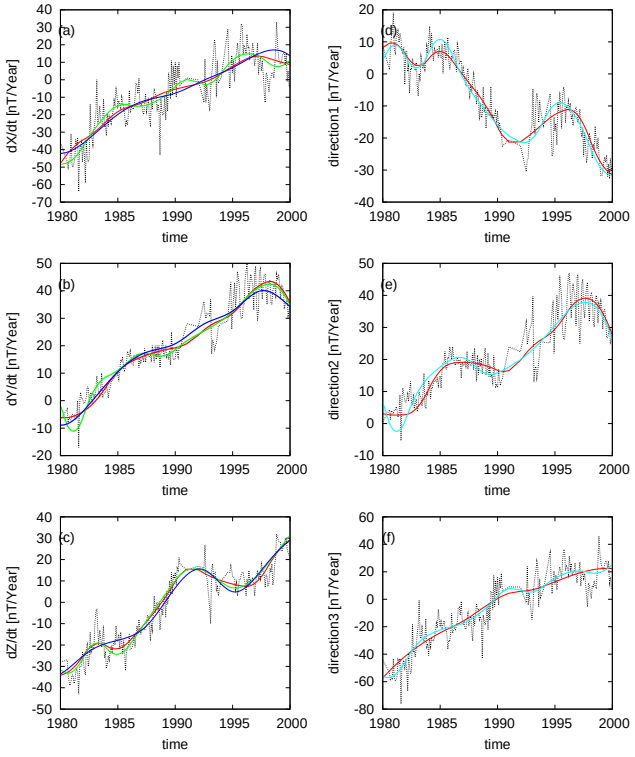

Figure 3: Same comparison as Fig. 2 but for Gnangara observatory (Australia) using the same line style.

component of Niemegk. Without considering the covariances, temporal details in $\dot{Y}$ variation are very closely fit, but when the covariance is considered, the behaviour is much simpler.

5. DISCUSSION

The sub-figures (d-f) of Fig.2 and Fig. 3 show plots the predictions of both models against the data in the directions of the eigenvectors of the Niemegk and Gnangara data covariance matrix, respectively. For Niemegk, the eigenvector with the lowest noise is predominantly made up of the $\dot{Y}$ component. The other two directions are combinations of $\dot{X}$ and $\dot{Z}$ respectively approximately perpendicular to and parallel to the mean effect of the ring current (including induced field). When the raw $(\dot{X}, \dot{Y}, \dot{Z})$ data are fit, both $\dot{X}$ and $\dot{Z}$ are noisy, but resolved into the frame of the eigenvectors, the direction perpendicular to the ring current effect has much lower noise, and therefore the model attempts a much closer fit to the data in this direction, as is clearly seen in the figure. This closer fit provides a strong constraint on model behaviour, as two components must be fit closely. This allows differentiation between internal and external sources, and so the very fine scale detail in $\dot{Y}$ is no longer fit, as to do so is inconsistent with fitting the intermediate eigenvector direction. Without this constraint, we might erroneously fit far too much detail in $\dot{Y}$, leading to an inappropriate interpretation as to what part of the secular variation can be explained by an internal field. Further, this constraint seems to simplify the detection of geomagnetic jerks, where they were not obvious before. Fig.3d provides evidence for 4 geomagnetic jerks in Gnangara happened between 1980 and 2000.

ACKNOWLEDGEMENTS

The authors would like to record their gratitude to S. Macmillan, N. Olsen and M. Mandea for providing data and many discussions. Further, Benoit Langlais and Gauthier Hulot, who organized the First Swarm meeting in Nantes. The work was funded by DFG SPP 1097.

REFERENCES

T. J. Sabaka, N. Olsen, and M. E. Purucker. Extending comprehensive models of the Earth's magnetic field with Ørsted and CHAMP data. *Geophys. J. Int.*, 159:521–547, 2004.

R. Holme and J. Bloxham. The treatment of attitude errors in satellite geomagnetic data. *Phys. Earth Planet. Int*, 98:221–233, 1996.

R. Holme and A. Jackson. The cause and treatment of

anisotropic errors in near-Earth geomagnetic data. *Phys. Earth Planet. Int*, 103:375–388, 1997.

I. Wardinski and R. Holme. A time–dependent model of the earth's magnetic field and its secular variation for the period 1980 to 2000. submitted to JGR, 2006.

C. de Boor. *A Practical Guide to Splines*. Springer-Verlag, New York, 1978.